ORIGINAL ARTICLE

UDC: 615.46::616.31
DOI: https://doi.org/10.2298/VSP191212014M

The advantages and disadvantages of biodentine: satisfactory mechanical properties and radiopacity not meeting ISO standard

Prednosti i nedostaci biodentina: zadovoljavajuća mehanička svojstva i radiološka vidljivost koja ne zadovoljava ISO standard

Sanja Milutinović-Smiljanić*, Dragan Ilić†, Vesna Danilović*, Djordje Antonijević‡

University of Belgrade, Faculty of Dental Medicine, *Department of Histology, †Clinic for Conservative Dentistry, Belgrade, Serbia; ‡University of Belgrade, Institute for Nuclear Science "Vinča", Laboratory for Atomic Physics, Belgrade, Serbia

Abstract

Background/Aim. In dentistry, the concept of using inert materials for tissue repair has been replaced by the strategy to find bioactive materials which positively interact with human tissues. The aim of this study was to characterize the physicochemical properties of the commercially available calcium silicate and calcium carbonate-based dental cement, biodentine (Septodont, France). **Methods.** Material elucidation included the measurements of radiopacity, scanning electron microscopy and x-ray dispersive analyses, wettability, Fourier transform infrared spectroscopy, microindentation, micro- to nanoporosity, setting time, pH and calcium ion release. The cells (mouse bone marrow mesenchymal stem cells – BMSCs) were grown on biodentine surface in order to evaluate its behaviour under biological conditions. **Results.** The radiopacity of the cement (2.8 mmAl) was below ISO requirement for a root canal filling material. The cement was composed of fine powder with particles similar in size and shape, changing from oval to cubic after having been soaked in a simulated body fluid. Biodentine demonstrated good micromechanical properties and low porosity attributed to microporosity with the average pore size of 92 μm. Wettability (contact angle = 41°), calcium ion release (0.098 μg/cm²) and pH of storage solution (9.07) showed satisfactory characteristics. The BMSCa in intimate contact with cement particles remained viable, indicating biodentine good biocompatibility. **Conclusion.** Biodentine exhibits good mechanical and physicochemical characteristics, but possesses insufficient radiopacity.

Key words:
tricalcium silicate; dental cements; materials, testing; x-ray microtomography.

Apstrakt

Uvod/Cilj. U stomatologiji, koncept primene inertnih materijala u cilju reparacije tkiva zamenjen je strategijom pronalaženja bioaktivnih materijala koji pozitvno deluju na humana tkiva. Cilj studije bio je karakterizacija fizičko-hemijskih osobina komercijalno dostupnog dentalnog cementa na bazi kalcijum silikata i kalcijum karbonata, biodentina (Septodont, Francuska). **Metode.** Ispitivanje materijala obuhvatilo je merenja radiografskog kontrasta, skening elektronsku mikroskopiju i radiografsku disperzivnu analizu, kvašenje, Furier-ovu transformocionu infracrvenu spektroskopiju, čvrstinu, mikro- i nano-poroznost, vremena vezivanja, pH vrednosti i oslobađanja kalcijumovih jona. Ćelije (mezenhimalne stem ćelije kostne srži miša – BMSCs) su uzgajane na površini biodentina sa ciljem da se ispita njegovo ponašanje u biološkim uslovima. **Rezultati.** Radiološki kontrast cementa (2.8 mm Al) bio je niži od ISO standarda za materijale namenjene punjenju kanala korena. Cement se sastojao od finog praha sa česticama male veličine i oblika koji se iz ovalnog menjao u kockasti nakon potapanja u simuliranu telesnu tečnost. Biodentin je pokazao dobre mikromehaničke osobine i nisku poroznost sa prosečnom veličinom pora 92 μm. Kvašenje (Ca = 41°), oslobađanje jona kalcijuma (0,098 μg/cm²) i pH rastvora gde je čuvan (9.07), pokazali su zadovoljavajuće karakteristike. BMSCs u neposrednom kontaktu sa cementnim česticama zadržale su vijabilnost što je ukazalo na dobru biokompatibilnost biodentina. **Zaključak.** Biodentin je ispoljio dobre mehaničke i fizičko-hemijske karakteristike, ali bez zadovoljavajućeg radiografskog kontrasta.

Ključne reči:
trikalcijum silikat; dentalni cementi; materijali, testiranje; mikrokompjuterizovana tomografija.

Correspondence to: Djordje Antonijević, University of Belgrade, Institute for Nuclear Science "Vinča", Laboratory for Atomic Physics, Mike Alasa 12-14, 11 000 Belgrade, Serbia. E mail: antonijevic@vin.bg.ac.rs

Introduction

Remarkable progress has been made over the last few decades in the field of materials science [1–3]. In dentistry, the concept of using inert materials for tissue repair has been replaced by the strategy to find bioactive materials which positively interact with human tissues [4, 5]. Numerous materials were manufactured with the goal to improve the treatment of pulp infection, which causes over five million interventions per year only in the United States [6, 7]. In this context, calcium silicate cements (CSC) were fabricated with the intention to replace mechanically weak calcium hydroxide materials used for healing of pulp lesions and orthograde/retrograde root canal filling. In order to meet the clinical requirements of CSC-based dental material, a radiopacifier has to be added to its composition to enable the visibility of cement on radiographs [2, 8, 9]. However, finding an ideal balance between the ratio of radiopacifier and cement powder remains a challenge of the dental and engineering community [3, 10, 11]. When choosing a proper radiopacifier for cement fabrication, several aspects should be taken into consideration. Namely, it should be biocompatible, which means that it does not damage the surrounding tissues, and it should be inert (meaning that it does not react with other cement compounds) [9, 12–16].

The first CSC-based dental material was introduced in 1993 by Torabinejad, as a mineral trioxide aggregate (MTA) [17] . This formulation consists of Portland cement and a radiopacifier bismuth oxide [Z(Bi) = 83] in 4 : 1 proportion. It was used effectively for root-end filling, pulp capping, apexification and root perforation repair [18, 19]. Nonetheless, MTA experiences some weaknesses including extended setting time (around two hours), washouts, staining of coronal dentine and impaired mechanical properties [2, 17, 20, 21]. Bismuth oxide is claimed as responsible for most of these downsides [22–24]. Therefore, a new formulation named biodentine (Septodont, Saint Maur, France) has been lunched recently [25–27]. It contains calcium silicate, calcium carbonate; zirconium oxide instead of bismuth oxide is added to improve material's radiopacity and calcium chloride is added in liquid component to reduce its setting time [13, 14]. Biodentine is considered superior to MTA due to higher biocompatibility of zirconium oxide in comparison to bismuth oxide and zirconium ability to increase the toughness of a material[16, 21, 28, 29]. Zirconium oxide is well-known in dentistry as a part of different forms of zirconia ceramics [17]. Unfortunately, in contrast to its superior biological and mechanical behavior, it has lower capacity than bismuth oxide to confer satisfactory radiopacity, due to the lower atomic number of zirconium (Z = 40) in comparison to bismuth (Z = 83) [30, 31].

Contradictory findings in the literature report biodentine to be as radiopaque as 2.8 mmAl [32], 4.1 mm Al [33], 1.5 mm Al [34], 2.06–2.52 mm Al [16] and 5.8 mm Al [35]. Therefore, there were some attempts to improve the radiopacity of biodentine by adding calcium tungstate ($BD+CaWO_4$) or zirconium oxide ($BD+ZrO_2$) [16].

This study was conducted to investigate physicochemical properties of biodentine, as well as its biocompatibility.

Methods

Material preparation

Biodentine specimens were prepared in accordance with the manufacturer's instructions. A capsule of biodentine was mixed with five drops of liquid component and placed in a mixing device Technomix (Lineatac, Italy) at the speed of 4000 rotations/min for 30 seconds.

Radiopacity determination

The radiopacity of the cements was calculated in accordance with the International Standard Organization (ISO) 6876 [36]. Five specimens for each testing procedure were made in accordance with the manufacturer's instructions and placed in teflon rings (1 mm × 8 mm). They were positioned on CCD radiovisiography (RVG)-based digital sensor (Trophy Radiology, Cedex, France) alongside an aluminum stepwedge varying in thickness from 1 mm to 10 mm, in 1 mm increments. An x-ray unit (Trophy Radiology) operating at 65 kV, 7 mA, a focus to target distance of 33.5 mm and exposure time of 0.074 s was used. Obtained digital images were analyzed using Trophy for Windows Software to make comparison between the grey scale values of the specimens and different thickness of the calibrated stepwedge.

Scanning electron microscopy (SEM) and energy dispersive x-ray analysis (EDX) of hydrated cements

Specimens of the hydrated cements were placed in a simulated body fluid (SBF) for two weeks, coated with gold and subjected to analysis using SEM (LEO 435 VP, LEO Electron Microscopy Ltd., Cambridge, England). In addition, scanning electron micrographs obtained in backscatter electron mode were used for x-ray dispersive analysis (EDX) to determine elemental constitution of the material. SBF was prepared from the following chemicals: 7.996 g NaCl, 0.350 g $NaHCO_3$, 0.224 g KCl, 0.228 g K2HPO4 x $3H_2O$, 0.305 g $MgCl_2$ x $6H_2O$, 0.278 g $CaCl_2$, 0.071 g Na_2SO_4 and 6.057 g $(CH_2OH)_3CNH_2$ and 1 l of ion exchanged water. The pH was set to 7.4 by stirring the solution with HCl.

Wettability measurements

Contact angle (CA) of glycerol (2 μL in volume) was measured by applying a sessile drop on six cement specimens. The profile of the liquid drops was recorded with contact angle analyzer ("Vinča" Institute, Belgrade, Serbia). Thereafter, CAs were calculated using Image J software by fitting the contour of the droplet placed on the surface (tangent method).

Fourier transform infrared (FTIR) spectroscopy

The hydrated specimens immersed in SBF for two weeks were desiccated and crushed into powder. Thereafter, the phase composition of the specimens was characterized by FTIR (Nicollet 380 FT-IR, Termo Electron Corporation) in attenuated total reflectance (ATR) mode. All peaks were assigned according to the established reference spectra.

Micromechanical measurements

Micromechanical characteristics of biodentine were evaluated by cyclic micro indentations using the Biodent 1000 Reference Point Indentation instrument (Active Life Scientific, Inc., Santa Barbara, CA) (RPI). Ten indentation cycles were performed on the cement surface at 2 Hz and the maximum force of 10 N. The following parameters were assessed: the 1st cycle indentation distance (ID 1st), indentation distance increase (IDI), total indentation distance (TID) and the average energy dissipated (Avg ED).

Micro- to nanoporosity analysis

For testing the microporosity, cements were kept for two months in SBF and scanned using micro-computed tomography (μCT) (Skyscan-Bruker 1172, Kontich, Belgium) operated at 100 kV, 100 μA, exposure time of 1150 ms, copper aluminum filter, rotating 180° in 0.4 steps, 5 μm isotropic resolution and 2,048 × 2,048 pixels per slice. Images were rebuilt using the NRecon v.1.6.9.8 software with beam hardening correction of 20%, ring artifact correction of 8%, post-alignment of -1 and smoothing of 1. For porosity assessment CTAn 1.14.4.1 software (Skyscan-Bruker) was used for all analyses. Threshold was set at the low mean value of 58 and the max of 255 to determine the following structural morphometric parameters: total porosity (%), closed porosity (%), open porosity (%) and pore size (μm).

For nanoporosity determination, specimens stored in SBF for two months were subjected to high-pressure mercury intrusion porosimetry (Carlo Erba Porosimeter 2000). It operated in the interval 0.1–200 MPa and Milestone 100 Software System was employed for the analysis.

Setting time determination

The initial setting time was determined at 60 s interval time using a 100 g indenter with a needle having a flat end of 2 mm in diameter. Material was considered set at the time when it was not possible to observe any mark on its surface.

Measurements of pH of storage solution and calcium ion release

For pH measurements, three cylindrical specimens (4 × 6 mm) were placed in hermetically sealed cylindrical polystyrene holders containing 25 mL of artificial saliva (Ca^{2+} concentration of saliva was 0.017 ± 0.005 kg/L at pH = 7.0) and maintained at 37 °C for two weeks. A pHmeter (WTW Ino Lab 1, Germany) with temperature-compensated electrode (WTW, Sen Tix 81, Germany) was used. For calcium ion release calculation, specimens were mixed with the artificial saliva (1 mL of saliva per 1 cm^2 specimen) and kept in an incubator at 37 °C for 14 days. Thereafter, the residue was dissolved with 10 mL of deionized water in a volumetric flask and subjected to the analysis by direct injection into an Inductively Coupled Plasma-Mass Spectrometer (ICP-MS) (Nexion 300X, PerkinElmer, CA, USA). The double-spike composition was defined relative to calcium (Calcium ICP Standard 1,000 mg/L Ca CertiPUR) standard and calibrated.

Cell culture and testing

For testing the cell adherence to cement surface, three specimens were sterilized and cultured for five days with mouse bone marrow mesenchymal stem cells (BMSCs). Cells were cultured in a low-glucose Dulbecco's modified Eagle's medium (DMEM) with 10% fetal bovine serum (FBS) and 1% penicillin/streptomycin (PS). The osteogenic medium for BMSCs consisted of the growth medium plus 100 nL dexamethasone, 10 mL β-glycerophosphate, 0.05 mL ascorbic acid and 10 nL 1α, 25-dihydroxyvitamin. Firstly, the presence of cells in media was confirmed using an optical microscope. Thereafter, the specimens with cells grown on their surfaces were fixed with 4% glutaraldehyde, dehydrated with different concentrations of ethanol (50 %, 60 %, 70 %, 80 %, 90 %, 95 % and 100%), dried at a critical point dryer for 30 min (critical point dryer bal tec CDP 030, Leica Microsysteme, Wetzlar, Germany), coated with gold and subjected to SEM observation.

Results

Figure 1 shows the results of radiopacity, EDX, wettability and FTIR measurements. Biodentine exhibited the radiopacity of 2.8 mm Al, while the glycerol droplet formed an average contact angle of 41°on its surface. EDX analysis revealed elemental peaks for the following elements: calcium, carbon, oxygen, sodium, aluminum, silicon, zirconium and chlorine. The FTIR spectrum indicated the presence of 3,414 cm^{-1} band corresponding to water molecules and Ca-OH groups in the structure. The band at 1,414 cm^{-1} can be assigned to the stretching vibrations of the carbonate group. The bands at 997 cm^{-1} and 983 cm^{-1} correspond to the Si-O stretching vibrations in Q2 site and lattice vibrations of tobermorite. The peak at 873 cm^{-1} can be assigned to out-of-plane vibrations of C-O bond, while the band at 712 cm^{-1} is typical of calcium carbonate.

Figure 2 depicts the SEM analysis of bioactivity experiment together with RPI outcomes. Having been soaked in SBF cement, crystals were transformed from round to cubic-like.

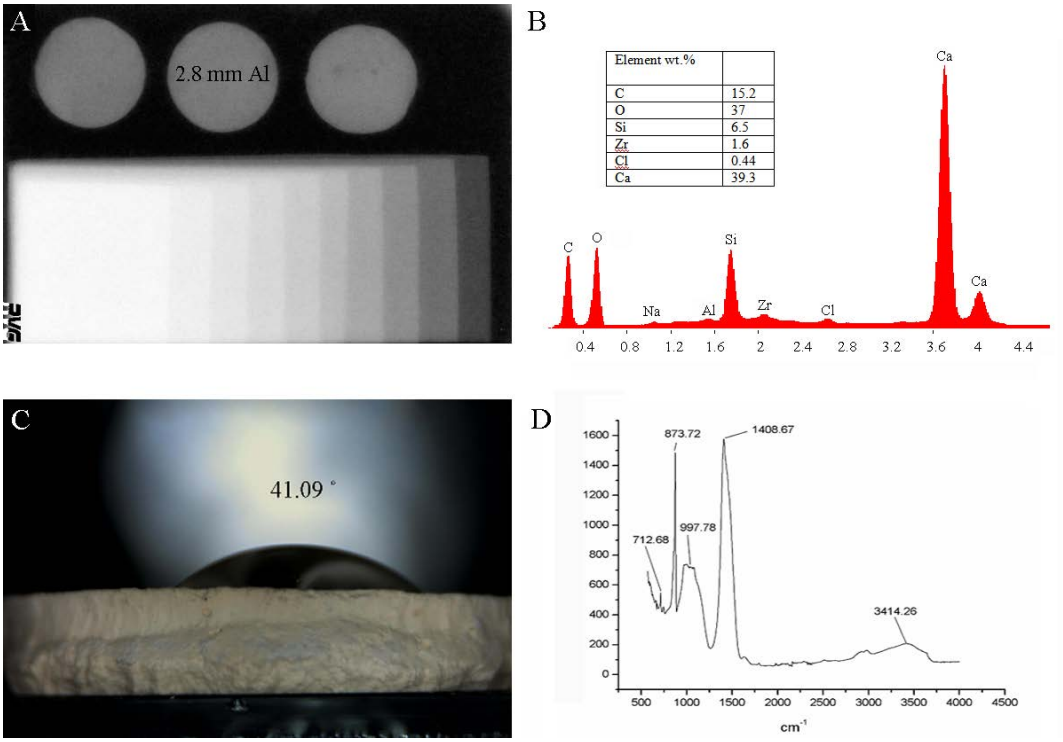

Fig. 1 – Physicochemical properties of biodentine: A) Radiopacity as expressed in equivalent thickness of aluminum showing cement specimens alongside an aluminum stepwedge; B) Energy dispersive x-ray analysis of hydrated cement specimen; C) Contact angle of glycerol droplet on cement surface; D) Fourier transform infrared spectroscopy of biodentine specimens after having been soaked in a simulated body solution for two weeks.

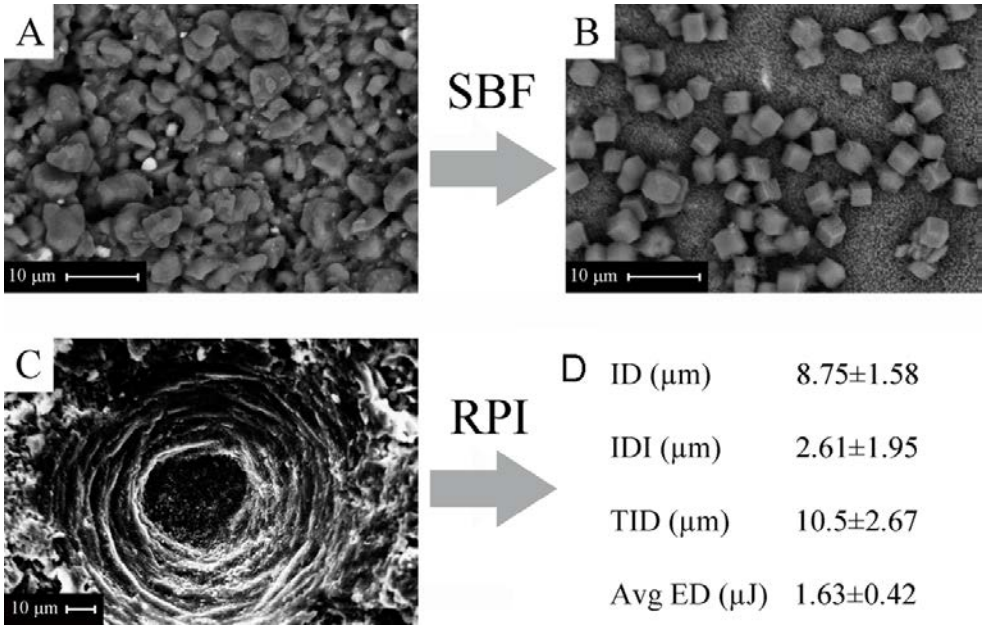

Fig. 2 – A, B) Morphology and surface precipitates of biodentine before and after having been soaked in a simulated body fluid; C, D) Scanning electron micrograph of indented cement specimen and reference point indentation outcomes of the measured parameters (results are shown as mean ± standard deviation).

Figure 3 reveals the findings of µCT measurements. Biodentine specimens exhibited low microporosity with the prevalence of closed pores. The analysis of pore size distribution demonstrated that 50% of the pores were in range between 10 and 49 µm. Figure 4 shows the results of nanoporosity analysis indicating almost total absence of nanopores in the cement structure after two months storage in SBF.

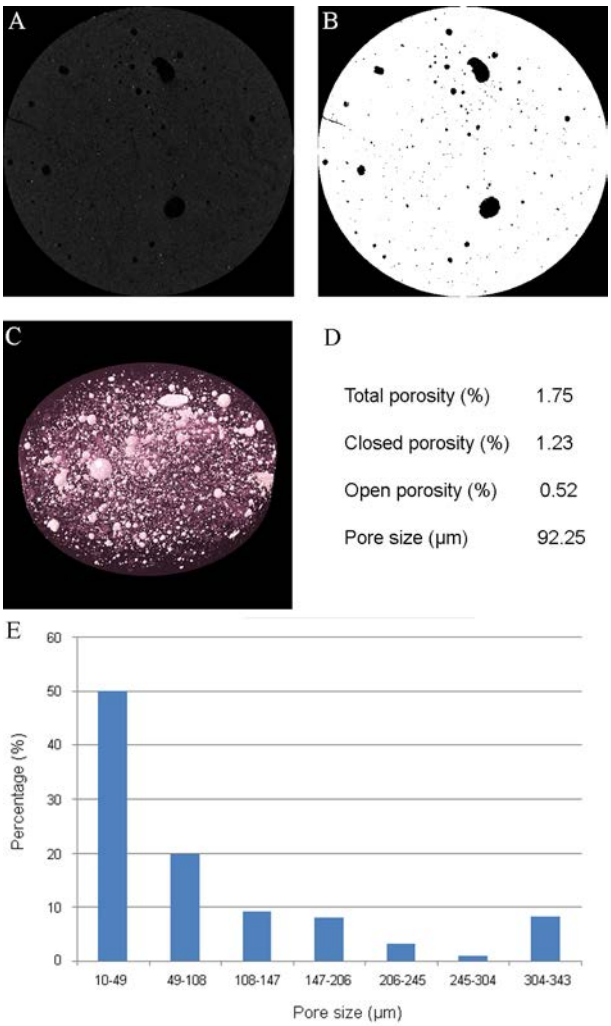

Fig. 3 – Micro-computed tomography measurements of biodentine porosity: A, B) Cross-sectional micro-computed tomographic slices; C) Three-dimensional volume rendering of biodentine; D) Results of microporosity measurements; E) Cement pore size distribution.

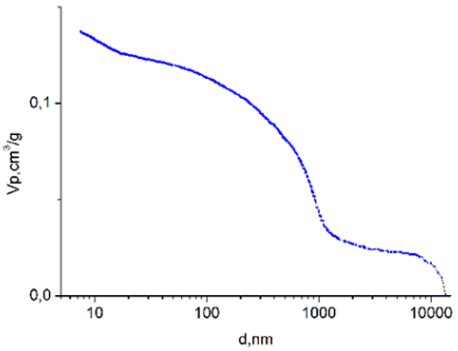

Nanoporosity	
Bulk density (g/cm^3)	2.37
Total sample porosity (%)	24.59
Pore radius average (nm)	432
Total cumulative vol.(mm^3/g)	137.4
Specific surface area (m^2/g)	6.32

Fig. 4 – Cumulative nanopore volumes obtained from mercury intrusion porosimetry measurements.

Table 1 reveals the results of initial setting time, pH of cement storage solution and calcium ion release.

Table 1

The results of initial setting time, pH value of specimen solution after the storage in a simulated body fluid for 14 days and the release of calcium ion after soaking specimens in artificial saliva for 14 days

Setting time (min, mean ± SD)	22 ± 2
pH	9.07
Calcium ion release (μg/cm²)	0.098

SD – standard deviation.

Figure 5 shows cells with numerous cytoplasmic processes attached to the cement surface after the 5-day incubation period. Cells infiltrated into pores with numerous cytoplasmic extensions.

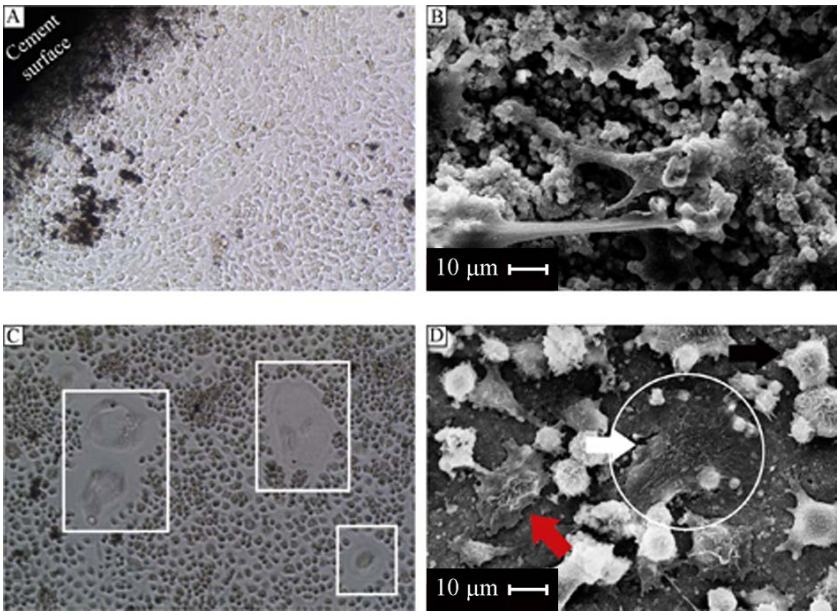

Fig. 5 – Cells attachment to biodentine surface: A) Optical microscopy of cell culture adjacent to cement surface, and B) cells adherence to cement crystals observed by scanning electron microscopy (SEM); C) Optical and D) SEM of cytoplasmic extensions on cement surface that indicate cell adhesion. Note the beginning of cement resorption caused by osteoclast-like cells (arrows).

Discussion

The long-standing goal in the field of CSC-based dental materials engineering is to find appropriate balance between the type and ratio of radiopacifier and cement powder [16]. This study encompassed biodentine's multilevel characterization, since this is the first formulation on the market incorporating zirconium oxide as a radiopacifying agent. All in all, although the results revealed quite satisfactory biological and microstructural properties of Bbodentine, its radiopacity did not meet the required criteria for adequate contrast between material and surrounding anatomical structures on radiographs.

The SEM analysis has shown that biodentine possesses the structure consisting of nano- to micro-scale particles of uniform shape. As it is known from materials science, structures composed of particles having similar size possess higher mechanical strength due to the enhanced potential for particles packing [30, 37] . In addition, microporosity of biodentine was 1.75ww%, which is lower than previously reported (6%) [24]. The analysis of μCT pores size distribution showed that 50% of micro pores were between 10 and 49 μm; on the other side mercury intrusion porosimetry did not show any presence of pores. Micro CT measurements enabled detecting pores higher than 5 μm, while mercury intrusion porosimetry allowed the determination of pores in the range of 7 nm to 15 μm. It can be additionally concluded that in the micropores ranging 10–49 μm most were greater than 15 μm. The lower porosity of the cement is a desirable quality, since it is related to higher mechanical performance of cement and because it leads to lower microleakage between root canal dentine and the material [22]. The lower cement porosity consequently leads to a lower micro gap between dentine and cement. Subsequently, a lower micro gap is associated with the avoidance of periradicular fluids to penetrate at tooth-cement interface and cause bacterial contamination [23].

Lower setting time of biodentine than previously reported for MTA comes as the consequence of finer cement particles and represents an important advantage for dental practitioners [23, 38]. The change in morphology from round shape to cubic-like crystals in SFB-soaked specimens confirmed that biodentine is modified during interaction with a biologically simulated system indicating its bioactivity – an ability of the material to provoke positive reaction from the host tissue [39]. Here, it is attributed to the potential of the cement to produce calcium carbonated crystals in the presence of SBF [10]. This was confirmed by FTIR spectra of the hy-

drated specimens having the calcium silicate phases transformed into tobermorite. In addition, calcium ion release is an indicator of biodentine's biointeractivity – an early interplay between cement surface and host tissue [40]. Finally, pH value of the solution was alkaline (9.07), which is also an important prerequisite for the successful healing of inflamed pulp tissue [6, 30]. All these favorable characteristics of biodentine were followed by cells adhering well to the cement surface. Also, biodentine induces reparative dentin synthesis and transforming growth factor beta 1 (TGF-β1) [7, 41]. To fully appreciate the significance of these and preceding findings, it may be useful to consider in more details whether biodentine may be used *in vivo* as a bone substitute material to fill bone defects after surgical procedures.

The average contact angle of reference liquid on biodentine was 41°. It has been reported during the recent years that osteoblasts preferentially adhere to the surfaces of biomaterials with the similar wettability to themselves [42]. Although glycerol was used instead of water and the literature data lack the knowledge about the wettability of CSC, this value is generally higher than reported for monolayer of bone-like proliferating cells (27°) and for nano-hydroxyapatite/chitosan bone cement (33.5°) [42]. A more recent research has shown the contact angle of distilled water on biodentine to be 25.3 ± 0.8°, indicating desirable hydrophobicity of the cement [35]. The factors affecting measured contact angles are material structural design and constitution, but divergences in the results may also arise from higher roughness of the materials, as shown in thorough and methodological study by Kisic et al. [39].

As measured by digital CCD-based radiography, the radiopacity of biodentine was equivalent to 2.8 mm Al, which is lower than minimum ISO requirement for radiopacity of an endodontic material (3 mm Al). This is in accordance with the results of Tanalp et al. [33], who reported that biodentine is as radiopaque as 2.8 mm Al, but in contrast with the findings of other authors where it exhibited the lower (1.5 mm Al [34] and 2.06– 2.52 mm Al [16]), and higher radiopacity value (4.1 mm Al [33] and 5.8. mm Al [35]) than ISO standard proposes. The differences could be due to various factors, such as various sensors for radiopacity determination [34]. The physical cause that explains different x-ray sensitivity of conventional film-based radiography and digital CCD-based sensor is the difference between the absorption of x-rays by silica and CCD sensor, silver and film emulsion, exposure time, tube voltage and source-to-object-distance [2, 31]. A material having similar composition to the detector absorbs most of the energies making the x-ray detector most sensitive. Thus, it appears more radiopaque in comparison to the material with different composition than the detector [43]. Having all the above-mentioned in mind, we concluded that more radiopacifier should be added to biodentine.

Conclusion

Despite satisfactory micromechanical characteristics of biodentine, it does not meet 3 mm Al ISO requirement for radiopacity, which is extremely significant for its clinical application. Therefore, the fabrication of CSC with adequate characteristics remains a challenge for the dental and engineering community.

Acknowledgements

The work was supported by the Ministry of Education, Science and technological development of the Republic of Serbia (Grant numbers III 45005: Functional, functionalized and advanced nanomaterials, and III 41013: Functional genomics of hypothalamus and medulla in hypertension induced by chronic stress).

Conflict of Interest

All authors declare that there is no conflict of interest.

R E F E R E N C E S

1. *Jokanović V, Čolović B, Marković D, Petrović M, Soldatović I, Antonijević D,* et al. Extraordinary biological properties of a new calcium hydroxyapatite/poly(lactide-co-glycolide)-based scaffold confirmed by in vivo investigation. Biomed Tech (Berl) 2017; 62(3): 295−306.
2. *Ćetenović B, Čolović B, Vasilijić S, Prokić B, Pašalić S, Jokanović V,* et al. Nanostructured endodontic materials mixed with different radiocontrast agents-biocompatib. J Mater Sci Mater Med 2018; 29(12): 190.
3. *Li Q, Hurt AP, Coleman NJ.* The Application of 29Si NMR Spectroscopy to the Analysis of Calcium Silicate-Based Cement using Biodentine as an Example. J Funct Biomater 2019; 10(2): pii: E25.
4. *Weber MT, Hannig M, Pötschke S, Höhne F, Hannig C.* Application of plant extracts for the prevention of dental erosion: an in situ/in vitro study. Car Res 2015; 49(5): 477–87.
5. *Mohamed DA, Fayyad DM.* The effect of different bioactive materials on the odontogenic differentiation potential of dental pulp stem cells using two different culture mediums. Tanta Dent J 2017; 14(3): 120–8.
6. *Kamal EM, Nabih SM, Obeid RF, Abdelhameed MA.* The reparative capacity of different bioactive dental materials for direct pulp capping. Dent Med Probl 2018; 55(2): 147−52.
7. *Cetenovic B, Prokic B, Vasilijic S, Dojcinovic B, Magic M, Jokanovic V*, et al. Biocompatibility Investigation of New Endodontic Materials Based on Nanosynthesized Calcium Silicates Combined with Different Radiopacifiers. J Endod 2017; 43(3): 425−32.
8. *Medigovic I, Antonijevic D.* In vitro radiographic density of dental posts measured by digital radiography. Oral Radiol 2014; 30: 9–12.
9. *Careddu R, Duncan HF.* How does the pulpal response to Biodentine and ProRoot mineral trioxide aggregate compare in the laboratory and clinic? Br Dent J 2018; 225: 743−9.
10. *Antonijevic D, Medigovic I, Zrilic M,Jokic B, Vukovic Z, Todorovic Lj.* The influence of different radiopacifying agents on the radiopacity, compressive strength, setting time, and porosity of Portland cement. Clin Oral Invest 2014; 18(6): 1597–604.
11. *Ilić D, Antonijević Dj, Biočanin V, Čolović B, Danilović V, Komlev V,* et al. Physico-chemical and biological properties of dental

calcium silicate cements - literature review. Hemijska industrija 2019; 73(5): 281−94.
12. *Liedke GS, Spin-Neto R, da Silveira HE, Wenzel A.* Radiographic diagnosis of dental restoration misfit: a systematic review. J Oral Rehabil 2014; 41(12): 957–67.
13. *Tuğ Kılkış B, Er K, Taşdemir T, Yildirim M, Taskesen F, Tümkaya L,* et al. Neurotoxicity of various root canal sealers on rat sciatic nerve: an electrophysiologic and histopathologic study. Clin Oral Investig 2015; 19(8): 2091–100.
14. *Liedke GS, Spin-Neto R, Vizzotto MB, Da Silveira PF, Silveira HE, Wenzel A.* Diagnostic accuracy of conventional and digital radiography for detecting misfit between the tooth and restoration in metal-restored teeth. J Prosth Dent 2015; 113(1): 39–47.
15. *Goracci C, Juloski J, Schiavetti R, Mainieri P, Giovannetti A, Vichi A, Ferrari M.* The influence of cement filler load on the radiopacity of various fibre posts ex vivo. Int Endod J 2015; 48(1): 60−7.
16. *Ochoa-Rodríguez VM, Tanomaru-Filho M, Rodrigues EM, Guerreiro-Tanomaru JM, Spin-Neto R, Faria G.* Addition of zirconium oxide to Biodentine increases radiopacity and does not alter its physicochemical and biological properties. J Appl Oral Sci 2019; 27: e20180429.
17. *Asgary S, Motazedian HR, Parirokh M, Eghbal MJ, Kheirieh S.* Twenty years of research on mineral trioxide aggregate: A scientometric report. Iran Endod J 2013; 8(1): 1–5.
18. *Choi Y, Park SJ, Lee SH, Hwang YC, Yu MK, Min KS.* Biological effects and washout resistance of a newly developed fast-setting pozzolan cement. J Endod 2013; 39(4): 467–72.
19. *Gandolfi MG, Taddei P, Siboni F, Modena E, Ginebra MP, Prati P.* Fluoride-containing nanoporous calcium-silicate MTA cements for endodontics and oral surgery: Early fluorapatite formation in a phosphate-containing solution. Int Endod J 2011; 44(10): 938–49.
20. *Marciano MA, Duarte MAH, Camilleri J.* Dental discoloration caused by bismuth oxide in MTA in the presence of sodium hypochlorite. Clin Oral Invest 2015; 19(9): 2201–9.
21. *Kaur M, Singh H, Dhillon JS, Batra M, Saini M.* MTA versus Biodentine: Review of literature with a comparative analysis. J Clin Diagn Res 2017; 11(8): ZG01−5.
22. *Sauia TS, Gomes BP, Pinheiro ET, Zaia AA, Ferraz CC, Souza-Filho JF.* Microleakage evaluation of intraorifice sealing materials in endodontically treated teeth. Oral Surg Oral Med Oral Pathol Oral Radiol Endod 2006; 102(2): 242−6.
23. *Camilleri J.* Characterization and hydration kinetics of tricalcium silicate cement for use as a dental biomaterial. Dent Mater 2011; 27(8): 836–44.
24. *De Souza ET, Nunes Tameirão MD, Roter JM, De Assis JT, De Almeida Neves A, De-Deus GA.* Tridimensional quantitative porosity characterization of three set calcium silicate-based repair cements for endodontic use. Micro Res Tech 2013; 76(10): 1093–8.
25. *Popović BM, Prokić B, Prokić BB, Jokanović V, Danilović V, Živković S.* Histological evaluation of direct pulp capping with novel nanostructural materials based on active silicate cements and biodentine on pulp tissue. Acta Vet (Beograd) 2013; 63: 347–60.
26. *Grazziotin-Soares R, Nekoofar MH, Davies TE, Bafail A, Alhaddar E, Hübler R et al.* Effect of bismuth oxide on white mineral trioxide aggregate: Chemical characterization and physical properties. Int Endod J 2014; 47(6): 520–33.
27. *Elnaghy AM.* Influence of acidic environment on properties of Biodentine and white mineral trioxide aggregate: A comparative study. J Endod 2014; 40(7): 953–7.
28. *Chang SW, Lee SY, Ann HJ, Kum KY, Kim EC.* Effects of calcium silicate endodontic cements on biocompatibility and mineralization-inducing potentials in human dental pulp cells. J Endod 2014; 40(8): 1194–200.
29. *Li M, Guo D, Ma T, Zhang G, Shi Y, Zhang X.* High fracture toughness in a hierarchical nanostructured zirconium. Mat Sci Eng A-Struct 2014; 606: 330–3.
30. *Bosso-Martelo R, Guerreiro-Tanomaru JM, Viapiana R, Berbert FL, Duarte MA, Tanomaru-Filho M.* Physicochemical properties of calcium silicate cements associated with microparticulate and nanoparticulate radiopacifiers. Clin Oral Invest 2016; 20(1): 83−90.
31. *Rakocevic Z.* Osnovi radiologije dento-maksilofacijalne regije. Principi i tehnike. Belgrade: Balkanski stomatološki forum; 1998. (Serbian)
32. *Camilleri J, Sorrentino F, Damidot D.* Investigation of the hydration and bioactivity of radiopacified tricalcium silicate cement, Biodentine and MTA Angelus. Dent Mater 2013; 29(5): 580–93.
33. *Tanalp J, Karapınar-Kazandağ M, Dölekoğlu S, Baybora Kayahan M.* Comparison of the radiopacities of different root-end filling and repair materials. ScientificWorldJournal. 2013; 2013: 594950.
34. *Kaup M, Schäfer E, Dammaschke T.* An in vitro study of different material properties of Biodentine compared to ProRoot MTA. Head Face Med 2015; 11: 16.
35. *Farrugia C, Lung CYK, Schembri Wismayer P, Arias-Moliz MT, Camilleri J.* The Relationship of Surface Characteristics and Antimicrobial Performance of Pulp Capping Materials. J Endod 2018; 44(7): 1115−20.
36. International Organization for Standardization. ISO 6876, Dental root canal sealing materials. 2nd ed. Geneva: 36. International Organization for Standardization; 2001.
37. *Saghiri MA, Gutmann JL, Orangi J, Asatourian A, Sheibani N.* Radiopacifier particle size impacts the physical properties of tricalcium silicate-based cements. J Endod 2015; 41(2): 225–30.
38. *Grech L, Mallia B, Camilleri J.* Investigation of the physical properties of tricalcium silicate cement-based root-end filling materials. Dent Mat 2013; 29(2): e20–8.
39. *Kisić D, Nenadović M, Štrbac S, Adnadjević B, Rakočević Z.* Effect of UV/ozone treatment on the nanoscale surface properties of gold implanted polyethylene. Appl Surf Sci 2014; 307: 311–8.
40. *Kumari S, Mittal A, Dadu S, Dhaundiyal A, Abraham A, Yendrembam B.* Comparative evaluation of physical and chemical properties of calcium silicate-based root-end filling materials (mineral trioxide aggregate and biodentine): An *in vitro* study. Indian J Dent Sci 2018; 10(4): 197−202.
41. *Laurent P, Camps J, About I.* Biodentine(TM) induces TGF-β1 release from human pulp cells and early dental pulp mineralization. Int Endod J 2012; 45(5): 439−48.
42. *Zou Q, Li Y, Zhang L, Zuo Y, Li J, Li X.* Characterization and cytocompatibility of nano-hydroxyapatite/chitosan bone cement with the addition of calcium salts. J Biomed Mater Res B Appl Biomater 2009; 90(1): 156−64.
43. *Rasimick BJ, Shah RP, Musikant BL, Deutsch AS.* Radiopacity of endodontic materials on film and a digital sensor. J Endod 2007; 33(9): 1098−101.

Received on December 12, 2019
Revised on January 22, 2020
Accepted on January 23, 2020
Online First February, 2020